POLISH
JOURNAL *of* RADIOLOGY

Review paper

Photon-counting computed tomography in radiology

Oktay Algin[1,2,3,A,D,E,F], Nazime Tokgoz[4,E,F], Filippo Cademartiri[5,B,D,E]

[1]Interventional MR Clinical R&D Institute, Ankara University, Ankara, Türkiye
[2]Department of Radiology, Medical Faculty, Ankara University, Ankara, Türkiye
[3]National MR Research Center (UMRAM), Bilkent University, Ankara, Türkiye
[4]Yıldırım Beyazıt University, Türkiye
[5]Fondazione Toscana Gabriele Monasterio per la Ricerca Medica e di Sanità Pubblica, Pisa, Toscana, Italy

Abstract

Photon-counting detector computed tomography (PCD-CT) devices have recently been introduced into practice, despite photon-counting detector technology having been studied for many years. PCD-CT devices are expected to provide advantages in dose reduction, tissue specificity, artifact-free imaging, and multi-contrast demonstration capacity. Noise reduction and increased spatial resolution are expected using PCD-CT, even under challenging scanning conditions. Some experimental or preliminary studies support this hypothesis. This pictorial review illustrates the features of PCD-CT systems, particularly in the interventional field. PCD-CT offers superior image quality and better lesion discrimination than conventional CT techniques for various conditions. PCD-CT shows significant improvements in many aspects of vascular imaging. It is still in its early stages, and several challenges have been identified. Also, PCD-CT devices have some important caveats. The average cost of these devices is 3 to 4 times higher than conventional CT units. This additional cost must be justified by improved clinical benefits or reduced clinical harms. Further investigations will be needed to resolve these issues.

Key words: photon counting detector (PCD), dose reduction, multi-contrast imaging, computed tomography (CT), artifact.

Introduction

In photon-counting detector computed tomography (PCD-CT) devices the electrical signals from the CT detectors where the X-rays are detected are converted into images by software. X-rays are indirectly converted into electrical signals by flat panel detectors in 2 stages. First, the X-rays are converted into visible light through a scintillator in the upper layer [1]. In the second step, the light is absorbed by the photodiode layer and converted into electrical charges that activate pixels in the amorphous silicon layer [2,3]. The charges of each pixel are read by the reader at the bottom of the detector, and digital data is generated [1]. This data is then processed to create a digital image on the monitor [2,3]. PCDs convert X-rays into electrical signals through a semiconductor diode without an intermediary medium [1]. This review evaluates the advantages and disadvantages of PCD-CT systems.

Technologies for photon-counting detectors

Features of the PCD chips

Depending on the material, the thickness of the semiconductor diode layer might range from 1.6 to 30 mm [4,5]. A high voltage is applied to the semiconductor diode, creating a cloud that quickly separates positive and negative charges when it absorbs an incoming X-ray photon [6]. The electronic reading circuit records the electrical pulse [6].

The semiconductor detector material in the PCD immediately converts X-ray photons into electron-hole pairs upon arrival [6,7]. PCDs generate an energy pulse proportional to the energy of each photon striking the detector element [8,9].

Noise reduction and contrast-to-noise ratio improvement

An ideal PCD might generate less noise than an ideal energy integrating detector (EID) [10]. Different energy photons have different weightings in PCDs. Even in this scenario, however, it is not possible to obtain the ideal contrast-to-noise ratio (CNR). Reduced tissue contrast at high energy is the source of this. To maximise the image's CNR, high-weight energies might be moved to lower energies. The CNR increases as a result [10].

The growing number of artifacts is a drawback of low-energy scanning [10]. Using noncontrast-material enhanced PCD-CT scanning of the human brain, the grey matter–white matter CNR increased by approximately 30% compared to the conventional CT technique [11]. Head and neck CT angiograms revealed 9% reduced picture noise compared with prior CT scans, according to Symons *et al.* [12].

The benefits of PCD have been noted in research conducted thus far. First, because of its high attenuation at low energies, such as calcium or iodine, ideal energy weighting can be attained [4,12]. Second, when used for low-dose imaging, PCDs outperform EIDs in terms of eliminating electronic noise. Electronic noise has very little effect on EIDs at high X-ray intensities. However, electronic noise can severely distort the image in low-dose imaging [13]. Image noise was reduced by up to 20% in human lungs using PCD-CT [14].

Resolution

The spatial resolution is related to the size of the detector element. This is approximately 1×1 mm² in EID systems. It is difficult to reduce the spatial resolution further due to the presence of a separator between the detector elements in the EID technique [10]. With this separator, the reflection of light photons in the scintillator is prevented [10]. In PCD, there is no such separator, and the detector element size can be reduced [15]. The detector element sizes for PCD-CT range from 0.11×0.11 mm² to 0.5×0.5 mm² [16,17]. With a smaller detector pixel size, fine details are seen in greater detail, while noise is reduced [18]. Factors affecting the quality of this detector are charge sharing and reflected X-rays, which reduce the efficiency due to fluorescent escape [16,17].

Material decomposition

Virtual monochromatic images (VMIs) can be processed to create virtual non-contrast or coloured images in the PCT technique [1]. Two or more equations are required to reconstruct an image at the desired energy level. With more energy measurements, less noisy images can be produced. The accurate measurement of the contrast material, crystals, or calculi is important for material separation [1,10,18]. Differentiation of the contrast agent was achieved by measuring 3 different materials [7]. Water, calcium, and contrast agents. Accurate measurement of these agents is possible with measurements at 3 or more energy levels [19]. EID and PCD units can be compared in terms of many factors affecting quality. Table 1 compares the 2 systems [20].

Experimental studies

Significant advantages, such as a decrease in dose, an increase in spatial/geometric resolution, and a decrease in artifacts/iodine, have been observed in the PCD-CT technique [10]. Similar noise levels were observed, but a 32% dose reduction was noted in images captured with PCD compared to the EID technique [19]. Giersch *et al.* [21] noted that the same image can be obtained with fewer photons, resulting in a 60% dose reduction. In PCDs, more data points are obtained by using smaller detector elements [22]. Although this creates more noise for each detector, the noise level drops considerably after the reconstruction algorithms. The PCD 0.25-mm detector mode exhibited 19% less image noise in phantom, animal, and human scans in a recent study [23].

It was concluded that breast PCD-CT provides high-quality images with the potential for breast cancer screening and causes little patient discomfort [24]. Another study involving 300 women using a single-counter PCD-CT concluded that breast PCD-CT provides high-quality images and is suitable for women who do not want breast compression during mammography [25].

PCD-CT significantly improved the detection of focal liver/pancreas lesions smaller than 1 cm, tumour invasion, or liver steatosis even in the presence of iron overload [15]. Using VMIs with low-keV, PCD-CT yields significantly improved objective and subjective quality of arterial-phase oncological imaging compared with EID-CT [26]. PCD-CT imaging can detect more pancreatic cysts than conventional EID-CT [15]. It may be helpful in accurately evaluating small structures, such as enhancing mural nodules [15].

High resolution is crucial when imaging the temporal bone. Small structures cannot be diagnosed accurately at low resolution [1]. Compared with PCD-CT and high-spatial-resolution EID detectors, which had a comb filter placed in front of them, PCD-CT reduced the radiation dose, enabling clear visualisation of middle ear bones [27]. Leng *et al.* [18] achieved improved image quality in lung imaging with PCD-CT systems. In another study, researchers evaluated lung nodules and kidney stones. They observed that PCD-CT showed higher resolution but also higher noise [28]. Another study concluded that PCD-CT allowed for more precise lung nodule characterisation compared to conventional CT [29].

Table 1. Comparisons between conventional energy integrating detectors (EIDs) and photon-counting detectors (PCDs) [20,22,61]

	EIDs	PCDs
Detector materials	Cadmium tungstate, gadolinium oxide, gadolinium oxysulfide.	Cadmium telluride, cadmium zinc telluride, silicon, gallium arsenide, chromium compensated gallium arsenide.
Detection mechanism	Energy integrates through a 2-step process involving an X-ray scintillator and a photodiode. The X-ray scintillator converts X-rays to visible light, and the photodiode converts visible light to an electric signal.	Energy is resolved using a single-step process that involves a semiconductor and the direct conversion of X-rays into an electric signal.
Spectral abilities	Inherently, there are no X-ray energy-resolving capabilities due to charge integration.	Photon events are counted and categorized in digital counters with user-defined energy thresholds.
Energy-resolving mechanism	X-rays are converted to visible photons, and visible photons are converted to electronic signals. Photon energy information is lost during this process.	X-ray photon interactions generate charge clouds (electron-hole pairs) in the semiconducting layer, producing a signal directly proportional to the photon energy.
Spatial resolution	Smaller detector pixels become less dose-efficient due to the finite-width septum required between them.	Smaller detector pixel sizes are possible because septa between detector pixels are not needed.
Electronic noise	Noticeable on conventional CT images at low doses of scanning of obese patients.	Can be excluded from the measured signal by selecting an energy threshold higher than the electronic noise floor.
Photon weighting	High-energy X-rays receive more weight than low-energy X-rays, which deteriorates the contrast between soft tissue and iodinated contrast material.	All photon energy levels are uniformly weighted, which enhances the contrast between soft tissue and iodinated contrast material.
Reduction of beam-hardening and metal artifacts	Metal artifact reduction algorithms can be used to mitigate these artifacts.	The high-energy bin images are much less affected by these artifacts. Algorithms can be used to reduce any remaining artifacts.
Multi-energy imaging	Requires dual-source, dual-tube potentials, dual acquisitions, dual detector layers, or dual beam filters to acquire the necessary dual-energy data.	Single-source, single-tube potential, single-acquisition, single-detector layer, single-filter simultaneous multi-energy acquisition is inherently possible.
High-resolution imaging	Radiation dose is inefficient due to comb or grid filters, or decreased detector fill factor caused by the need for additional septa.	Radiation dose-efficient high-spatial-resolution imaging is possible due to inherently smaller detector pixels.
Energy-selective imaging	Limited options due to a lack of energy discrimination.	Energy binning enables K-edge imaging tailored to gadolinium, gold, bismuth, ytterbium, and other high-Z contrast agents.

CT angiography (CTA) has replaced digital subtraction angiography (DSA) for first-line vascular imaging in routine clinical practice [30]. Fast 3D isotropic data with high-resolution acquisition is important in CTA [15,30]. PCD-CT will be useful for imaging vessels and the detection of thrombosis with optimal doses (Figures 1 and 2) [15]. Lower extremity ischaemia and below-knee artery calcification cannot be optimally evaluated using conventional CT scans due to insufficient spatial resolution. PCD-CT overcomes these issues thanks to its multi-energetic nature by reducing streak artifacts and improving signal uniformity [31,32].

The major cause of spontaneous intracranial hypotension (SIH) is cerebrospinal fluid (CSF) leakage. Most CSF fistulas are usually 1-2 mm in diameter. Detecting small fistulas is challenging. PCD-CT can detect CSF fistulas more effectively than standard clinical imaging [10,33].

Distinguishing tumour invasion is crucial for the tumour staging of laryngeal and hypopharyngeal carcinoma [34]. However, the density of the unossified laryngeal cartilage is similar to the tumour structure in conventional CT scans, making it difficult to distinguish [34]. In such cases, PCD-CT can facilitate diagnosis [34]. In addition, PCD-CT provides better delineation of fractures, oedema, malignant involvement, and/or degenerative changes in bones and cartilage (Figure 3) [1].

Artifacts and quality factors

The higher the quality of the image, the less distortion there is. Artifacts are one of the factors that degrade image quality. The effect of artifacts on the image is analysed in various situations and systems. CNRs of iodine were similar in 120 kV EID and 140 kV PCD scans [4]. Pourmorteza et al. [35] compared the values of 120-kV EID and 140-kV PCD based on abdominal scans. Good agreement was observed between the Hounsfield units [35].

PCD-CT eliminates beam-curing artifacts. By obtaining VMIs, the optimum CNR and iodine concentration maps can be obtained [12,36]. These data were used to distinguish intravascular contrast media from calcified plaques in the carotid arteries [31]. CT imaging may be hindered by artifacts in patients with calcified plaques, metallic im-
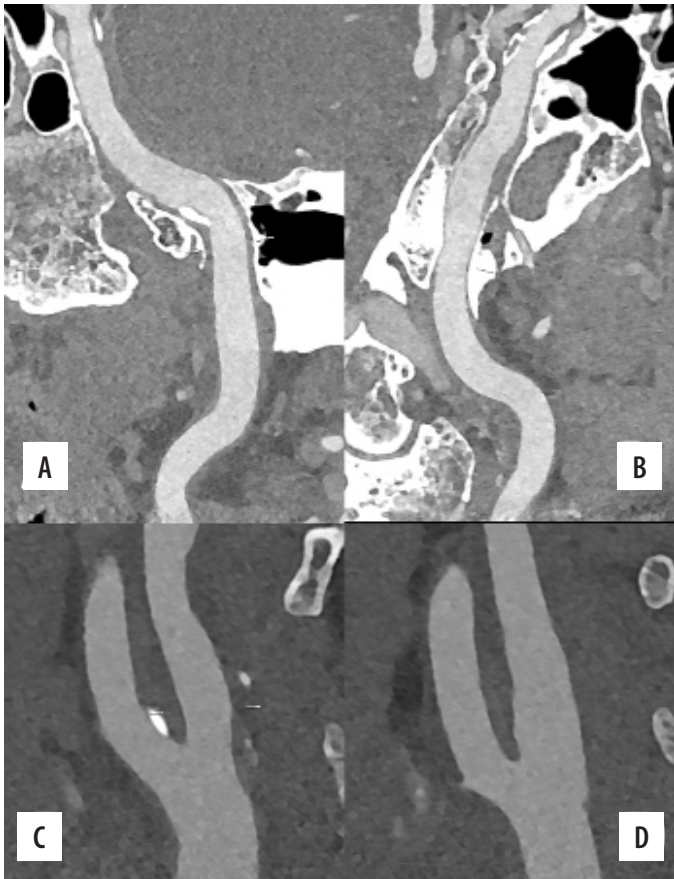
Figure 1. Photon-counting computed tomography (PCCT) angiography example of the intra-cranial arteries and carotid arteries with mild atherosclerosis. The figure shows the intrapetrous internal carotid arteries (**A, B**) with a curved multiplanar reconstruction along the central lumen line; the bilateral bifurcation of the carotid arteries is displayed in **C** (right) and **D** (left). The scan was performed on a commercial whole-body dual-source photon-counting CT scanner (Naeotom Alpha, Siemens Healthineers, Forchheim, Germany) with 0.2 mm slice thickness, 0.1 mm reconstruction increment, and FOV 140 mm. The images are displayed with a resolution matrix of 1024 × 1024 pixels on the source axial reconstructions with a kernel filtering of Bv60 (vascular kernel medium-sharp) and with the maximum intensity of Quantum Iterative Reconstruction (QIR 4). The actual displayed resolution is 0.1 mm (100 microns)
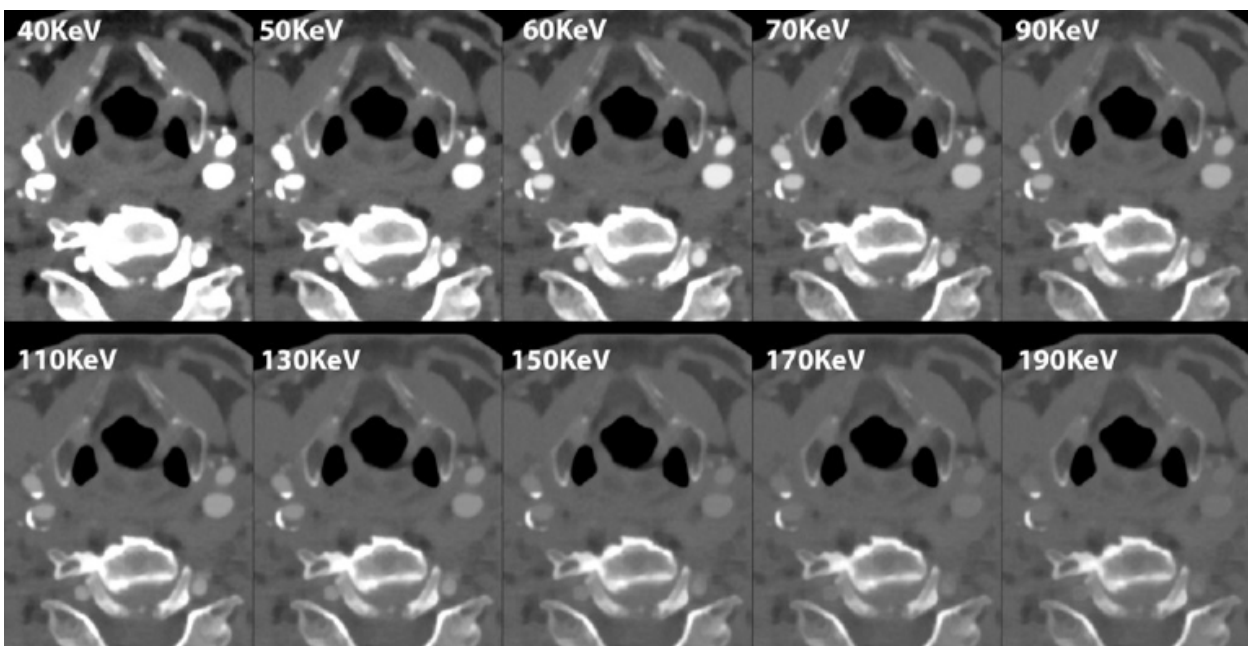

Figure 2. Photon-counting detector–computed tomography (PCD-CT) spectral angiography example of the carotid arteries with mild atherosclerosis. The figure shows spectral multi-energy axial reconstructions of carotid arteries at the level of the bifurcation; it is possible in this image to see the effect of increasing KeV directly within the standard acquisition. The scan was performed on a commercial whole-body dual-source photon-counting CT scanner (Naeotom Alpha, Siemens Healthineers, Forchheim, Germany) with 0.4 mm slice thickness, 0.2 mm reconstruction increment, and FOV 140 mm. The images are displayed with a resolution matrix of 1024 × 1024 pixels on the source axial reconstructions with a kernel filtering of Bv56 (vascular kernel medium-sharp) and with the maximum intensity of quantum iterative reconstruction (QIR 4)

plants, clips, and/or coils [37]. Metallic artifact reduction algorithms and VMIs have enhanced the image quality in PCD-CT [1,38,39]. This is especially crucial when assessing small stents made of highly attenuating materials. Recent research indicates that PCD-CT provides greater visibility and resolution of coronary lesions (Figure 4) [40,41].
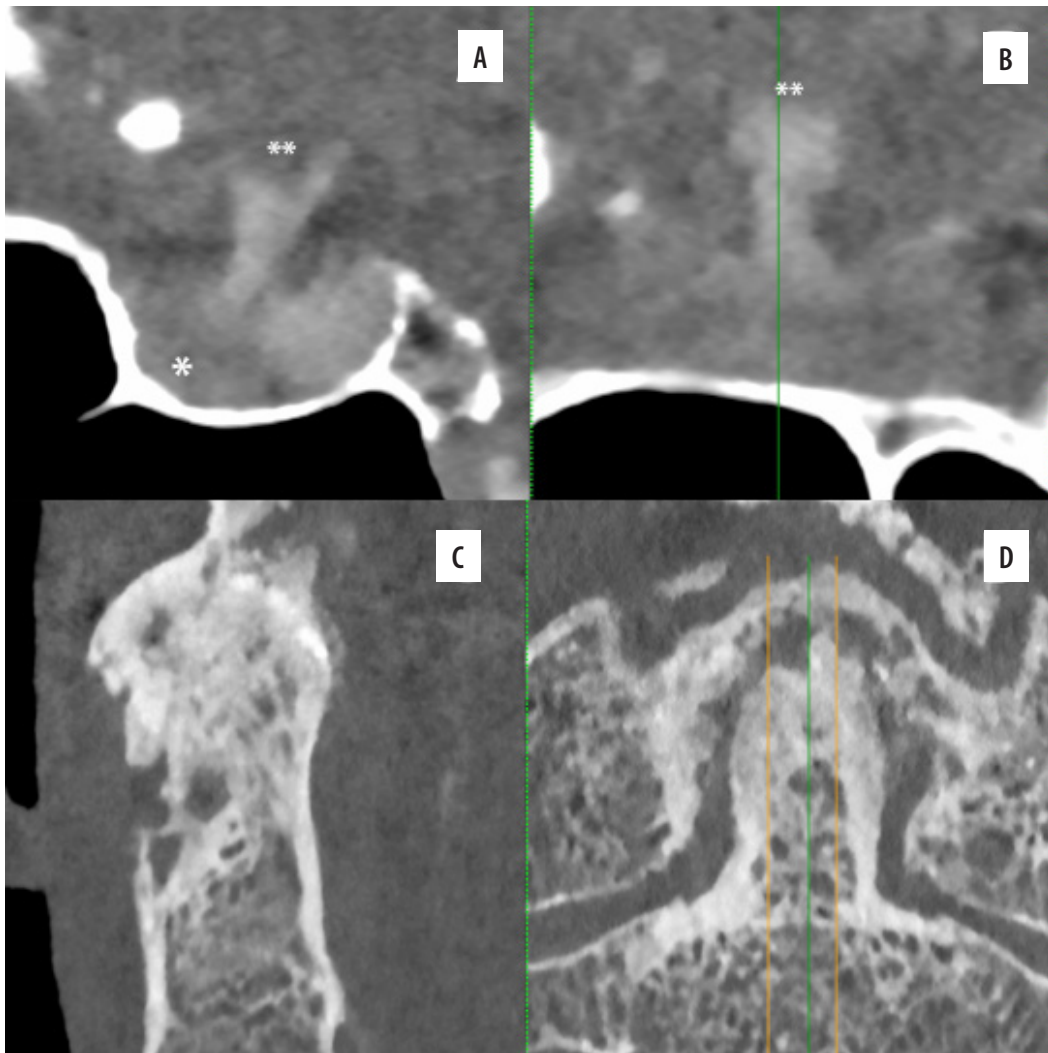
Figure 3. Photon-counting computed tomography (PCCT) examples of neuro applications. The figure shows the hypothalamus (**) the hypophyseal pedicle, and the hypophysis (*; anterior hypophysis) in sagittal (**A**) and coronal (**B**) planes; in **C** and **D** a sagittal and coronal view of high-resolution of the epistropheus tooth with severe degenerative alterations. The scan was performed on a commercial whole-body dual-source photon-counting CT scanner (Naeotom Alpha, Siemens, Germany) with 0.2 mm slice thickness, 0.1 mm reconstruction increment, and FOV 140 mm. The images are displayed with a resolution matrix of 1024 × 1024 pixels on the source axial reconstructions with a kernel filtering of Bv60-80 (vascular kernel medium-sharp) and with the maximum intensity of quantum iterative reconstruction (QIR 4). The actual displayed resolution is 0.1 mm (100 microns)

Images acquired by PCD-CT showed a significant reduction in metal artifacts and an increase in dose efficiency compared with EID-CT [42,43]. Additionally, fewer streaking artifacts were observed in PCD units [44].

Contrast agents

Tiny vessels of hypervascular lesions, arteriovenous malformations, haemangiomas, and neoplasms can be better visualised using PCD-CT angiography [10,15]. It may also improve the CNRs, allowing for a reduction in the iodine load. The use of non-iodinated and multiple contrast agents is among the advantages that PCD-CT can provide [22]. PCD-CT allows for the removal of iodine, thereby creating virtual non-contrast images similarly to dual-energy CT [10,15].

In individuals with renal insufficiency, reducing the iodine dose is crucial. Low monochromatic image usage in dual-energy CT and reduced tube voltage in conventional CT are 2 techniques for reducing the iodine load [45-47]. PCD-CT generates monoenergetic reconstructions through energy-resolved detection and is more useful for iodine-based contrast agent detection than conventional CT detectors [48]. Iodine-specific applications might enhance the quality of coronary artery imaging (Figure 5) [31]. VMIs obtained with 40-60 keV were the best for the detection of pulmonary embolism by quantitative metrics [48]. VMIs at 60–70 keV provided better image quality in terms of vessel contrast [15].

Although dual-energy CT has poor spectral separation, making it challenging to use alternative contrast agents, it does allow for various contrast agents [37,49]. In addition to iodine, barium, and gadolinium, PCD-CT can utilise high atomic number elements as contrast agents [30,37,48,49-52]. Materials that could be considered for PCD-CT include gold, platinum, xenon, bismuth, lutetium, tungsten, silver, and ytterbium [30,50-54].
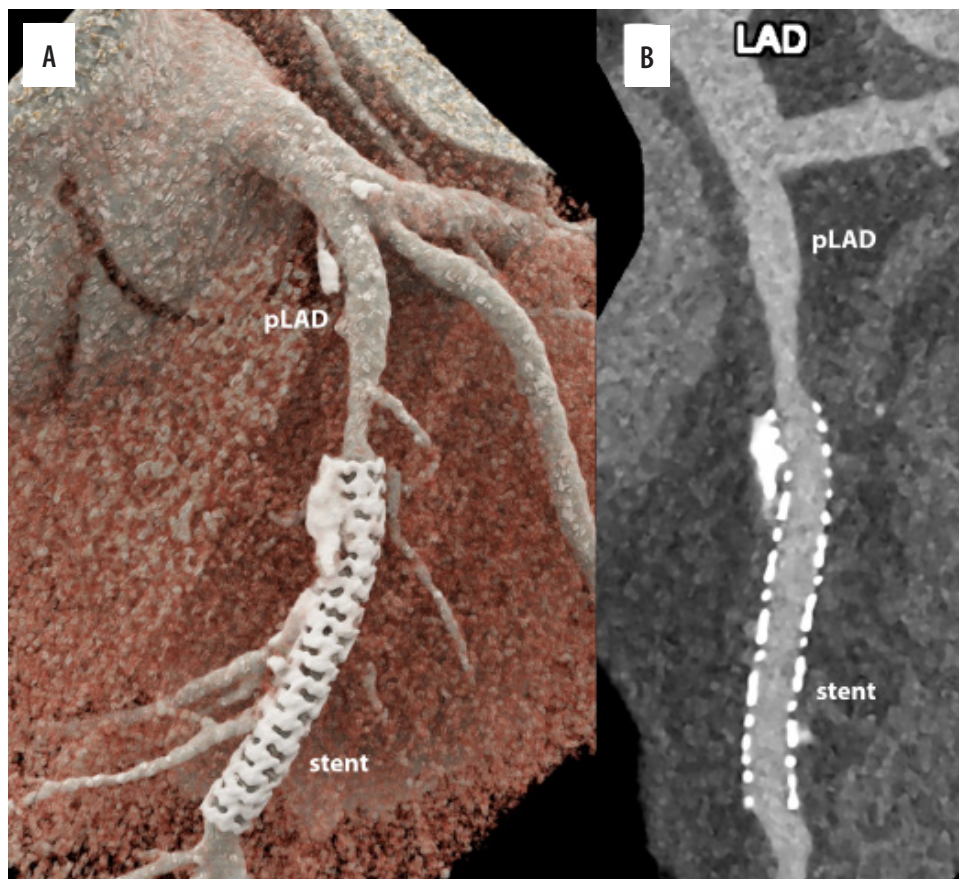
Figure 4. Cardiac/coronary photon-counting computed tomography (PCCT) example of a diseased coronary artery treated with an intracoronary stent. In the 2 main panels a 3D Cinematic Rendering (**A**), a curved multiplanar (MPR) reconstruction along the central lumen line of proximal (**B**; pLAD) and mid left anterior descending (**B**; stent). The scan was performed on a commercial whole-body dual-source photon-counting CT scanner (Naeotom Alpha, Siemens Healthineers, Forchheim, Germany) with 0.2 mm slice thickness, 0.1 mm reconstruction increment, and FOV 140 mm; the scan was performed with retrospective ECG gating with tube current modulation. In this case, the pLAD shows severe non-obstructive disease with non-calcified and calcified components down to the proximal edge of the coronary stent; the stent is perfectly patent and visible; stent struts are perfectly visible, and it is quite easy to assess the proximal calcification on the outer contour of the stent determining no issues in terms of intrastent lumen assessment. The images are displayed with a resolution matrix of 1024×1024 pixels on the source axial reconstructions with a kernel filtering of Bv76 (vascular kernel medium-sharp) and with the maximum intensity of quantum iterative reconstruction (QIR 4). The actual displayed resolution is 0.1 mm (100 microns)

It is fascinating to consider the potential use of novel contrast agents specifically designed for PCD-CT [6,30]. Gold-labelled nanoparticles have been the subject of many studies [53,54]. These metals are present in such small amounts that traditional CT scans cannot detect them. K-edge imaging and PCD-CT can be utilised for the identification and measurement of gold nanoparticles [30,53,54]. Even in the presence of additional contrast agents, such as iodine, they remain distinguishable [55].

Molecular CT imaging requires addressing safety concerns, including toxicity, stability, and patency, in addition to functionality issues, such as particle concentrations and size uniformity [6]. The distribution of particles and contrast material can be used to facilitate early cancer diagnosis [19,56]. Furthermore, the characterisation of the composition of atherosclerotic plaques can be enhanced using this method [57]. It is possible to differentiate between calcifications and iodine using dual-energy CT. It is simpler to distinguish between materials such as calcium and iodine by PCD-CT that have significant variations in their effective atomic numbers [10,18]. Dual-energy CT faces challenges in differentiating between fibrous and fatty tissues due to their significantly lower effective atomic number differences [58]. PCD-CT devices can be used to address this problem. Better material separation with enhanced spatial and temporal resolution, along with the use of targeted contrast agents, are the advantages of PCD-CT [37].

Due to PCD-CT's ability to differentiate between different contrast agents, K-edge imaging can display various contrast materials simultaneously. As a result, it might be possible to apply multiple contrast agents simultaneously and display their distinct distribution. Targeted nanoparticles and contrast agents, such as iodine or gadolinium, can be administered simultaneously [59]. It is possible to simultaneously inject several types of nanoparticles targeting various tissue types [6]. Moreover, imaging can be performed concurrently, and multiple contrast agents can be applied at different times [53,60]. Removing the contrast agents from the images can reconstruct non-contrast material-enhanced reformatted images [61]. Mul-
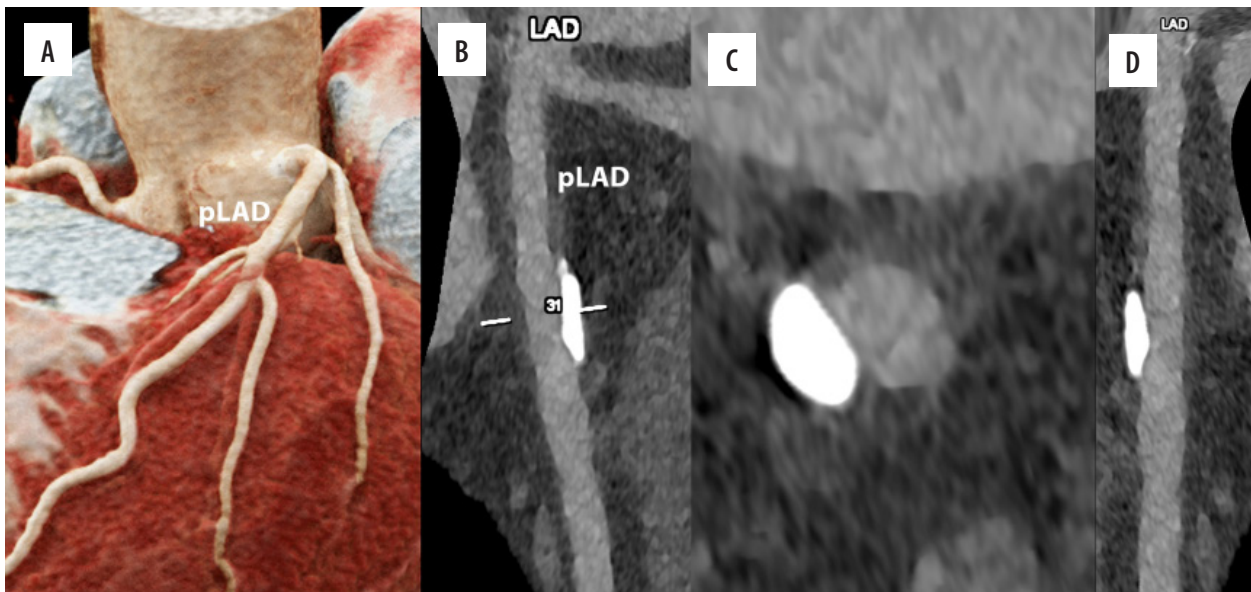
Figure 5: Cardiac/coronary photon-counting detector–computed tomography (PCD-CT) example of mildly diseased coronary arteries. In the 4 main panels a 3D cinematic rendering (**A**), a curved multiplanar (MPR) reconstruction along the central lumen line of proximal left anterior descending (**B**; pLAD), an MPR axial/cross-sectional view of the same vessel (**C**) and a stretched MPR view are displayed. The scan was performed on a commercial whole-body dual-source photon-counting CT scanner (Naeotom Alpha, Siemens, Forchheim, Germany) with 0.2 mm slice thickness, 0.1 mm reconstruction increment, matrix 1024 × 1024, kernel Bv60, and FOV 140 mm; the scan was performed with retrospective ECG gating with tube current modulation. In this case, the segments of coronary arteries show a large singular eccentric calcification of the pLAD with no effect on lumen patency (no lumen diameter or area reduction) and it is displayed with a resolution matrix of 1024 × 1024 pixels on the source axial reconstructions with a kernel filtering of Bv60 (vascular kernel medium-sharp) and with maximum intensity of quantum iterative reconstruction (QIR 4). The actual displayed resolution is 0.1 mm (100 microns)

tiple contrast agents can be effectively separated *in vivo* simultaneously using PCD-CT. Additionally, detecting bone marrow lesions or oedema is possible using virtual non-calcium images [61]. This approach reduces the radiation dose and eliminates the need for multiphase CT scans [12,14].

There are some limitations for PCD-CT systems. These limitations include increased costs, the need for larger computational, operating, or maintenance capabilities, the requirement for additional training on new acquisition/reconstruction algorithms, kernels, and technical challenges (such as charge sharing, pixel crosstalk, and pulse pile-up) [1,10]. The charge-sharing or pile-up phenomenon may lead to inaccuracies in data interpretation and reduced image quality [61]. These factors hinder the widespread use of PCD-CT scanners. In various clinical scenarios, there is a lack of data on the sensitivity and specificity of the new reconstruction algorithms, kernels, or spectral data sets [1]. Therefore, it is essential to develop and standardise high-resolution modes or scanning protocols for different body parts and specific issues [15,22].

Conclusions

PCD-CT has not yet been widely used in clinical practice, but preliminary results are promising. Among the promis-

ing features provided by PCDs are improved spatial resolution, material distinction, vessel delineation, and the ability to co-administer/apply different contrast agents. The radiation dose may be significantly reduced by PCD-CT compared to conventional EID-CT units. The fact that various quantitative maps that typically require multiple scans can now be generated with just one scan, thanks to the use of different contrast agents, indicates a reduction in dosage. Increased resolution leads to more detailed images, enabling earlier diagnosis and more accurate follow-up. Stents, coils, and vessels can be visualised more effectively with artifact reduction using PCD-CT systems and their dedicated software. PCD-CT has tremendous potential, but studies of its diagnostic ability and clinical utility for many disorders or body parts are currently limited. Further research and experience are needed before its benefits can be fully understood.

Disclosures

1. Institutional review board statement: Not applicable.
2. Assistance with the article: None.
3. Financial support and sponsorship: None.
4. Conflicts of interest: None.

References

1. Bette S, Risch F, Becker J, Popp D, Decker JA, Kaufmann D et al. Photon-counting detector CT – first experiences in the field of musculoskeletal radiology. Fortschr Röntgenstr 2024. DOI: 10.1055/a-2312-6914.

2. Lanca L, Silva A. Digital radiography detectors: a technical overview. Digital imaging systems for plain radiography. Springer, NY; 2013, pp. 9-19.

3. Spahn M. Flat detectors and their clinical applications. Eur Radiol 2005; 15: 1934-1947.

4. Gutjahr R, Halaweish AF, Yu Z, Leng S, Yu L, Li Z, et al. Human imaging with photon counting-based computed tomography at clinical dose levels: contrast-to-noise ratio and cadaver studies. Invest Radiol 2016; 51: 421-429.

5. Persson M, Huber B, Karlsson S, Liu X, Chen H, Xu C, et al. Energy-resolved CT imaging with a photon-counting silicon-strip detector. Phys Med Biol 2014; 59: 6709-6727.

6. Taguchi K, Iwanczyk JS. Vision 20/20: single photon counting x-ray detectors in medical imaging. Med Phys 2013; 40: 100901. DOI: 10.1118/1.4820371.

7. Willemink MJ, Persson M, Pourmorteza A, Pelc NJ, Fleischmann D. Photon-counting CT: technical principles and clinical prospects. Radiology 2018; 289: 293-312.

8. Ballabriga R, Campbell M, Llopart X. An introduction to the Medipix family ASICs. Radiation Measurements 2020; 136: 106271. DOI: https://doi.org/10.1016/j.radmeas.2020.106271.

9. Talla PT. Investigation of photon counting pixel detectors for X-ray spectroscopy and imaging. Doctoral dissertation, Friedrich-Alexander-Universität Erlangen-Nürnberg; 2011.

10. Toia GV, Mileto A, Borhani AA, Chen GH, Ren L, Uyeda JW, et al. Approaches, advantages, and challenges to photon counting detector and multi-energy CT. Abdom Radiol (NY) 2024; 49: 3251-3260.

11. Pourmorteza A, Symons R, Reich DS, Bagheri M, Cork TE, Kappler S, et al. Photon-counting CT of the brain: in vivo human results and image-quality assessment. AJNR Am J Neuroradiol 2017; 38: 2257-2263.

12. Symons R, Reich DS, Bagheri M, Cork TE, Krauss B, Ulzheimer S, et al. Photon-counting computed tomography for vascular imaging of the head and neck: first in vivo human results. Invest Radiol 2018; 53: 135-142.

13. Luhta R, Chappo M, Harwood B, Mattson R, Salk D, Vrettos C. A new 2D-tiled detector for multislice CT. In: Flynn MJ, Hsieh J (eds.). Proceedings of SPIE: medical imaging – physics of medical imaging. Bellingham, Wash: International Society for Optics and Photonics; 2006, p. 61420U.

14. Symons R, Pourmorteza A, Sandfort V, Ahlman MA, Cropper T, Mallek M, et al. Feasibility of dose-reduced chest CT with photon-counting detectors: initial results in humans. Radiology 2017; 285: 980-989.

15. Onishi H, Tsuboyama T, Nakamoto A, Ota T, Fukui H, Tatsumi M, et al. Photon-counting CT: technical features and clinical impact on abdominal imaging. Abdom Radiol (NY) 2024. DOI: 10.1007/s00261-024-04414-5.

16. Xu C, Danielsson M, Bornefalk H. Evaluation of energy loss and charge sharing in cadmium telluride detectors for photon-counting computed tomography. IEEE Trans Nucl Sci 2011; 58: 614-625.

17. Rajbhandary PL, Hsieh SS, Pelc NJ. Effect of spatial-energy correlation in PCD due to charge sharing, scatter, and secondary photons. In: Flohr TG, Lo JY, Gilat Schmidt T (eds.). Proceedings of SPIE: Medical Imaging – physics of medical imaging. Bellingham, Wash: International Society for Optics and Photonics; 2017, p. 101320.

18. Leng S, Yu Z, Halaweish A, Kappler S, Hahn K, Henning A, et al. Dose-efficient ultrahigh-resolution scan mode using a photon counting detector computed tomography system. J Med Imaging (Bellingham) 2016; 3: 043504. DOI: 10.1117/1.JMI.3.4.043504.

19. Roessl E, Proksa R. K-edge imaging in x-ray computed tomography using multibin photon counting detectors. Phys Med Biol 2007; 52: 4679-4696.

20. Leng S, Bruesewitz M, Tao S, Rajendran K, Halaweish AF, Campeau NG, et al. Photon-counting detector CT: system design and clinical applications of an emerging technology. Radiographics 2019; 39: 729-743.

21. Giersch J, Niederlöhner D, Anton G. The influence of energy weighting on x-ray imaging quality. Nucl Instrum Methods Phys Res A 2004; 531: 68-74.

22. Stein T, Rau A, Russe MF, Arnold P, Faby S, Ulzheimer S, et al. Photon-counting computed tomography – basic principles, potenzial benefits, and initial clinical experience. Fortschr Röntgenstr 2023; 195: 691-698.

23. Pourmorteza A, Symons R, Schöck F, et al. Image quality assessment and dose-efficiency of quarter-millimeter photon-counting CT of humans: first in vivo experience [abstr]. In: Radiological Society of North America scientific assembly and annual meeting program. Oak Brook, Ill: Radiological Society of North America; 2017.

24. Berger N, Marcon M, Saltybaeva N, Kalender WA, Alkadhi H, Frauenfelder T, et al. Dedicated breast computed tomography with a photon-counting detector: initial results of clinical in vivo imaging. Invest Radiol 2019; 54: 409-418.

25. Berger N, Marcon M, Frauenfelder T, Boss A. Dedicated spiral breast computed tomography with a single photon-counting detector: initial results of the first 300 women. Invest Radiol 2020; 55: 68-72.

26. Graafen D, Müller L, Halfmann M, et al. Photon-counting detector CT improves quality of arterial phase abdominal scans: a head-to-head comparison with energy-integrating CT. Eur J Radiol 2022. DOI: 10.1016/j.ejrad.2022.110514.

27. Leng S, Yu Z, Halaweish A, Kappler S, Hahn K, Henning A, et al. A high-resolution imaging technique using a whole-body, research photon counting detector CT system. In: Kontos D, Flohr TG (eds.). Proceedings of SPIE: Medical Imaging 2016 – physics of medical imaging. Bellingham, Wash: International Society for Optics and Photonics; 2016, p. 97831.

28. Leng S, Gutjahr R, Ferrero A, Kappler S, Henning A, Halaweish A, et al. Ultra-high spatial resolution, multi-energy CT using photon counting detector technology. In: Flohr TG, Lo JY, Gilat Schmidt T (eds.). Proceedings of SPIE: Medical Imaging – physics of medical

imaging. Bellingham, Wash: International Society for Optics and Photonics; 2017, p. 101320Y.

29. Zhou W, Montoya J, Gutjahr R, Ferrero A, Halaweish A, Kappler S, et al. Lung nodule volume quantification and shape differentiation with an ultra-high resolution technique on a photon counting detector CT system. Proc SPIE Int Soc Opt Eng 2017; 11: 10132. DOI: 10.1117/12.2255736.

30. Chen H, Xu C, Persson M, Danielsson M. Optimization of beam quality for photon-counting spectral computed tomography in head imaging: simulation study. J Med Imaging (Bellingham) 2015; 2: 043504. DOI: 10.1117/1.JMI.2.4.043504.

31. Cau R, Saba L, Balestrieri A, Meloni A, Mannelli L, La Grutta L, et al. Photon-counting computed tomography in atherosclerotic plaque characterization. Diagnostics (Basel) 2024; 14: 1065. DOI: 10.3390/diagnostics14111065.

32. Meloni A, Frijia F, Panetta D, Degiorgi G, De Gori C, Maffei E, et al. Photon-counting computed tomography (PCCT): technical background and cardio-vascular applications. Diagnostics (Basel) 2023; 13: 645. DOI: 10.3390/diagnostics13040645.

33. Schwartz FR, Malinzak MD, Amrhein TJ. Photon-counting computed tomography scan of a cerebrospinal fluid venous fistula. JAMA Neurol 2022; 79: 628-629.

34. Kuno H, Onaya H, Iwata R, Kobayashi T, Fujii S, Hayashi R et al. Evaluation of cartilage invasion by laryngeal and hypopharyngeal squamous cell carcinoma with dual-energy CT. Radiology 2012; 265: 488-496.

35. Pourmorteza A, Symons R, Sandfort V, Mallek M, Fuld MK, Henderson G, et al. Abdominal imaging with contrast-enhanced photon-counting CT: first human experience. Radiology 2016; 279: 239-245.

36. Alvarez RE. Near optimal energy selective x-ray imaging system performance with simple detectors. Med Phys 2010; 37: 822-841.

37. Wang AS, Hsieh SS, Pelc NJ. Dual-energy and multienergy techniques in vascular imaging. In: Saveden C, Rudin S (eds.). Cardio-vascular and Neuromuscular Imaging: Physics and Technology. Boca Raton, Fla: CRC; 2015, pp. 191-202.

38. Schmitt N, Wucherpfennig L, Rotkopf LT, Sawall S, Kauczor HU, Bendszus M, et al. Metal artifacts and artifact reduction of neurovascular coils in photon-counting detector CT versus energy-integrating detector CT – in vitro comparison of a standard brain imaging protocol. Eur Radiol 2023; 33: 803-811.

39. Nasirudin RA, Mei K, Penchev P, Fehringer A, Pfeiffer F, Rummeny EJ, et al. Reduction of metal artifact in single photon-counting computed tomography by spectral-driven iterative reconstruction technique. PLoS One 2015; 10: e0124831. DOI: 10.1371/journal.pone.0124831.

40. Sandfort V, Symons R, Cork TE, Bluemke DA, Pourmorteza A. 250 micron resolution photon-counting CT: potential for improved imaging of calcified coronary artery stenoses [abstr]. In: Radiological Society of North America scientific assembly and annual meeting program. Oak Brook, Ill: Radiological Society of North America; 2017, p. 139.

41. Bratke G, Hickethier T, Bar-Ness D, Bunck AC, Maintz D, Pahn G, et al. Spectral photon-counting computed tomography for coronary stent imaging: evaluation of the potential clinical impact for the delineation of in-stent restenosis. Invest Radiol 2020; 55: 61-67.

42. Do TD, Sawall S, Heinze S, Reiner T, Ziener CH, Stiller W, et al. A semi-automated quantitative comparison of metal artifact reduction in photon-counting computed tomography by energy-selective thresholding. Sci Rep 2020; 10: 21099. DOI: 10.1038/s41598-020-77904-3.

43. Zhou W, Bartlett DJ, Diehn FE, Glazebrook KN, Kotsenas AL, Carter RE, et al. Reduction of metal artifacts and improvement in dose efficiency using photon counting detector CT and tin filtration. Invest Radiol 2019; 54: 204-211.

44. Yu Z, Leng S, Kappler S, Hahn K, Li Z, Halaweish AF, et al. Noise performance of low-dose CT: comparison between an energy integrating detector and a photon-counting detector using a whole-body research photon-counting CT scanner. J Med Imaging (Bellingham) 2016; 3: 043503. DOI: 10.1117/1.JMI.3.4.043503.

45. Muenzel D, Bar-Ness D, Roessl E, Blevis I, Bartels M, Fingerle AA, et al. Spectral photon-counting CT: initial experience with dual-contrast agent K-edge colonography. Radiology 2017; 283: 723-728.

46. Dong J, Wang X, Jiang X, Gao L, Li F, Qiu J, et al. Low-contrast agent dose dual-energy CT monochromatic imaging in pulmonary angiography versus routine CT. J Comput Assist Tomogr 2013; 37: 618-625.

47. Machida H, Tanaka I, Fukui R, Shen Y, Ishikawa T, Tate E, et al. Dual-energy spectral CT: various clinical vascular applications. Radiographics 2016; 36: 1215-1232.

48. Yu Z, Leng S, Jorgensen SM, Li Z, Gutjahr R, Chen B, et al. Evaluation of conventional imaging performance in a research whole-body CT system with a photon-counting detector array. Phys Med Biol 2016; 61: 1572-1595.

49. Mongan J, Rathnayake S, Fu Y, Wang R, Jones EF, Gao DW, et al. In vivo differentiation of complementary contrast media at dual-energy CT. Radiology 2012; 265: 267-272.

50. Leng S, Zhou W, Yu Z, Halaweish A, Krauss B, Schmidt B, et al. Spectral performance of a whole-body research photon counting detector CT: quantitative accuracy in derived image sets. Phys Med Biol 2017; 62: 7216-7232.

51. Fornaro J, Leschka S, Hibbeln D, Butler A, Anderson N, Pache G, et al. Dual- and multi-energy CT: approach to functional imaging. Insights Imaging 2011; 2: 149-159.

52. Müllner M, Schlattl H, Hoeschen C, Dietrich O. Feasibility of spectral CT imaging for the detection of liver lesions with gold-based contrast agents: a simulation study. Phys Med 2015; 31: 875-881.

53. Jaffer FA, Weissleder R. Seeing within: molecular imaging of the cardiovascular system. Circ Res 2004; 94: 433-445.

54. Cormode DP, Skajaa T, Fayad ZA, Mulder WJ. Nanotechnology in medical imaging: probe design and applications. Arterioscler Thromb Vasc Biol 2009; 29: 992-1000.

55. Si-Mohamed S, Cormode DP, Bar-Ness D, Sigovan M, Naha PC, Langlois JB, et al. Evaluation of spectral photon counting computed tomography K-edge imaging for determination of gold nanoparticle biodistribution in vivo. Nanoscale 2017; 9: 18246-18257.

56. Barber WC, Wessel JC, Nygard E, Iwanczyk JS. Energy dispersive CdTe and CdZnTe detectors for spectral clinical CT and NDT applications. Nucl Instrum Methods Phys Res A 2015; 784: 531-537.

57. Meng B, Cong W, Xi Y, De Man B, Yang J, Wang G. Model and reconstruction of a K-edge contrast agent distribution with an x-ray photon-counting detector. Opt Express 2017; 25: 9378-9392.

58. Barreto M, Schoenhagen P, Nair A, Amatangelo S, Milite M, Obuchowski NA, et al. Potential of dual-energy computed tomography to characterize atherosclerotic plaque: ex vivo assessment of human coronary arteries in comparison to histology. J Cardiovasc Comput Tomogr 2008; 2: 234-242.

59. Schirra CO, Brendel B, Anastasio MA, Roessl E. Spectral CT: a technology primer for contrast agent development. Contrast Media Mol Imaging 2014; 9: 62-70.

60. Cormode DP, Si-Mohamed S, Bar-Ness D, Sigovan M, Naha PC, Balegamire J, et al. Multicolor spectral photon counting computed tomography: in vivo dual contrast imaging with a high count rate scanner. Sci Rep 2017; 7: 4784. DOI: 10.1038/s41598-017-04659-9.

61. Mourad C, Gallego Manzano L, Viry A, Booij R, Oei EHG, Becce F, et al. Chances and challenges of photon-counting CT in musculoskeletal imaging. Skeletal Radiol 2024; 53: 1889-1902.